Supplemental Materials and Methods

RNA extraction, reverse transcription (RT) and real-time PCR. Total RNA from cultured cells was extracted using the Trizol reagent (Invitrogen, Carlsbad, CA) as the manufacturer instructed. cDNAs were amplified and quantified in Bio-Rad CFX qRT-PCR detection system (Applied Biosystems Inc., Foster City, CA, USA), using FastStart Universal SYBR Green Master (ROX; Roche, Toronto, ON, Canada). Expression data were normalized to the geometric mean of housekeeping gene *GAPDH* to control the variability in expression levels and calculated as $2^{-[(C_t \text{ of gene}) - (C_t \text{ of } GAPDH)]}$, where C_t represents the threshold cycle for each transcript.

Immunohistochemistry (IHC). Paraffin-embedded tissues were analyzed using IHC with AGK antibody (Epitomics, Burlingame, CA, 1:500), p-STAT3 (Tyr705) antibody (Cell Signaling, Danvers, MA, 1:400), p-JAK2 (1007-1008) antibody (Epitomics, Burlingame, CA, 1:200). The degree of immunostaining of formalin-fixed, paraffin-embedded sections were reviewed and scored separately by two independent pathologists uninformed of the histopathological features and patient data of the samples. The scores were determined by combining the proportion of positively-stained tumor cells and the intensity of staining. The scores given by the two independent pathologists were combined into a mean score for further comparative evaluation. Tumor cell proportions were scored as follows: 0, no positive tumor cells; 1, <10% positive tumor cells; 2, 10%–35% positive tumor cells; 3, 35%–75% positive tumor cells; 4, >75% positive tumor cells. Staining intensity was graded according to the following standard: 1, no staining; 2, weak staining (light yellow); 3, moderate staining (yellow brown); 4, strong staining (brown). The staining index (SI) was calculated as the product of the staining intensity score and the proportion of positive tumor cells. Using this method of assessment, we evaluated protein expression in benign esophageal epithelia and malignant lesions by determining the SI, with possible scores of 0, 2,

3, 4, 6, 8, 9, 12, and 16. Samples with a SI ≥ 8 were determined as high expression and samples with a SI < 8 were determined as low expression. Cutoff values were determined on the basis of a measure of heterogeneity using the log-rank test with respect to overall survival.

Primers and Oligonucleotides

Used for subcloning and plasmid construction:	
HA tagged JAK2 and JAK2 fragments	
JAK2-UP	GCCGGATCCGCCATGTACCCATACGACGTCCCAGACT ACGCTGGAATGGCCTGCCTTACGAT
JAK2-DN	GGCGCGGCCGCTCATCCAGCCATGTTATCCCTTATTT GATCCAC
JH1-UP	GCCGGTACCGCCATGTACCCATACGACGTCCCAGACT ACGCTTTGTTTACTCCAGATTA
JH1-DN	GGCGAATTCTCATCCAGCCATGTTATCCC
JH2-UP	GCCGGATCCGCCATGTACCCATACGACGTCCCAGACT ACGCTGTGTTTCACAAAATCAG
JH2-DN	GGCGAATTCTCAACTGTTAAGATCTCGTATG
JH3-7-UP	GCCGGTACCGCCATGTACCCATACGACGTCCCAGACT ACGCTATGGGAATGGCCTGCCTTAC
JH3-7-DN	GGCGGATCCTCACATTTGGTTCATATGAGTAGG
Flag tagged AGK	
pSin Flag-AGK-up	GCCGGATCCGCCATGGACTACAAGGACGACGATGA CAAGACGGTGTTCTTTAAAACGCT
pSin Flag-AGK-dn	GGCACTAGTTCACTGGGTGGGGCTTGTGAGCATC
shRNA	
pSuper Retro AGK-RNAi#1-up	GATCCCCGGAGAGACCAGTAGTTTGATTCAAGAGAT CAAACTACTGGTCTCTCCTTTTTA
pSuper Retro AGK-RNAi#1-dn	AGCTTAAAAAGGAGAGACCAGTAGTTTGATCTCTTG AATCAAACTACTGGTCTCTCCGGG
pSuper Retro	GATCCCCGAGGCTACCTTCAGTAAGATTCAAGAGAT

AGK-RNAi#2-up	CTTACTGAAGGTAGCCTCTTTTTA
pSuper Retro AGK-RNAi#2-dn	AGCTTAAAAAGAGGCTACCTTCAGTAAGATCTCTTG AATCTTACTGAAGGTAGCCTCGGG
pSuper Retro JAK2-RNAi#1-up	GATCCCCGAAATATATTGGTGGAGAATTCAAGAGAT TCTCCACCAATATATTTCTTTTTA
pSuper Retro JAK2-RNAi#1-dn	AGCTTAAAAAGAAATATATTGGTGGAGAATCTCTTG AATTCTCCACCAATATATTTCGGG
pSuper Retro JAK2-RNAi#2-up	GATCCCCGCCAGAAACTTGAAACTTATTCAAGAGAT AAGTTTCAAGTTTCTGGCTTTTTA
pSuper Retro JAK2-RNAi#2-dn	AGCTTAAAAAGCCAGAAACTTGAAACTTATCTCTTG AATAAGTTTCAAGTTTCTGGCGGG
pSuper Retro STAT3-RNAi-up	GATCCCCGCACAATCTACGAAGAATCAATTCAAGAG ATTGATTCTTCGTAGATTGTGCTTTTTA
pSuper Retro STAT3-RNAi-dn	AGCTTAAAAAGCACAATCTACGAAGAATCAATCTCT TGAATTGATTCTTCGTAGATTGTGCGGG
AGK G126E mutation	
pSin Flag-AGK-G126E-up	GATCATTGTTGCAGGAGGAGATGAGACACTGCAGGA GGTTGTTACTG
pSin Flag-AGK-G126E-dn	CAGTAACAACCTCCTGCAGTGTCTCATCTCCTCCTGC AACAATGATC
His-tagged AGK	
pET-19b AGK-up	GCCCATATGATGACGGTGTTCTTTAAAACGCTTCG
pET-19b AGK-dn	GGCGGATCCTCACTGGGTGGGGCTTGTGAGCATCTG
Luciferase reporter	
pTAL STAT3-Luc-up	CGCGTGCTTCCCGAATTCCCGAATTCCCGAATTCCC GAATTCCCGAATTCCCGAACGTG
pTAL STAT3-Luc-dn	GATCCACGTTCGGGAATTCGGGAATTCGGGAATTCG GGAATTCGGGAATTCGGGAAGCA
Used for qPCR	
AGK-up	CTTGACAGGCTGCTCTCCTT
AGK-dn	GGAAGAAAACTACAGCTGGGC
ABCG2-up	TGGTGTTTCCTTGTGACACTG
ABCG2-dn	TGAGCCTTTGGTTAAGACCG
SOX2-up	GCTTAGCCTCGTCGATGAAC
SOX2-dn	AACCCCAAGATGCACAACTC

OCT4-up	GGTTCTCGATACTGGTTCGC
OCT4-dn	GTGGAGGAAGCTGACAACAA
NANOG-up	ATGGAGGAGGGAAGAGGAGA
NANOG-dn	GATTTGTGGGCCTGAAGAAA
BMI1-up	TCGTTGTTCGATGCATTTCT
BMI1-dn	CTTTCATTGTCTTTTCCGCC
ABCB7-up	TTGCCTTTTCCCAATCTCTG
ABCB7-dn	AGTGGAGGCCACATCAACTC
TLS-up	TCATGACGTGATCCTTGGTC
TLS-dn	CAGCAGTGGTGGCTATGAAC
RPA1-up	AGCTTCCATTCTGCGGC
RPA1-dn	GGCAATCCAGTGCCCTATAA
IGF2BP1-up	TTTCGGATTTGAATTTTCCG
IGF2BP1-dn	AGGCCATCGAAACTTTCTCC
IGF2BP2-up	CAGGTGAGGAGGGATGTTTC
IGF2BP2-dn	AAAGTGGAATTGCATGGGAA
SLC25A6-up	GATGCCCTTGTACTGCTTGTC
SLC25A6-dn	GCCGCCATCTCCAAGAC
C14orf166-up	TGCATTGTCAGCAGTTTTTGA
C14orf166-dn	TGACTGGCTTCTTGGTTTAGC
siRNA	
siABCB7	CGGTGGAGAACTAGATTTA
siTLS	CGAACAGGATAATTCAGACAA
siRPA1	GTCATCAACATCCGTCCCATT
siIGF2BP1	CCTGGCCCATAATAACTTTGT
siIGF2BP2	CGGATCTTTGGGAAACTGAAA
siSLC25A6	CGACAAGCAGTACAAGGGCAT
siC14orf166	GCAGTTGCTAAGGCAAATCAA
Used for EMSA probe	
STAT3-up	TCGACATTTCCCGTAAATC
STAT3-dn	GATTTACGGGAAATGTCGA
OCT-1-up	TGTCGAATGCAAATCACTAGAA
OCT-1-dn	TTCTAGTGATTTGCATTCGACA

Supplemental Figure Legends

Supplemental Figure 1. Mass-spectrometric peptide sequencing of JH2-interacting proteins and identification of their effects on STAT3 transcriptional activity. **(A)** Representative mass spectrometry plots and sequences of the peptides from potent JH2-interacting proteins identified from the JH2 precipitate presented in Figure 1A. **(B)** Expression of mRNA and STAT3 luciferase reporter activity following silencing of potent JH2-interacting proteins identified from the JH2 precipitate presented in Figure 1A. Error bars represent the mean ±SD of three independent experiments, * $P < 0.05$.

Supplemental Figure 2. AGK expression correlates with STAT3 activity in ESCC datasets. GSEA plot showing significant correlations between AGK expression and the STAT3-activated gene signatures (DAUER_STAT3_TARGETS_UP, V$STAT3_01/02) or STAT3-suppressed gene signatures (DAUER_STAT3_TARGETS_Dn) in a published cohort of ESCC gene expression profiles (statistic performed within tumor tissues from GSE20347/29001/33426, $n = 109$).

Supplemental Figure 3. Overexpression of AGK enhances the strength and duration of STAT3 activation. **(A-H)** Western blotting analysis of the expression of p-STAT3 (Tyr705) and total STAT3 in the indicated cells treated with IL-6 (1 ng/ml) for various times (0-480 min). GAPDH was used as a loading control.

Supplemental Figure 4. AGK promotes the stem cell population and stem cell-like phenotype in ESCC. Representative images of spheres formed by AGK transduced- or AGK silenced-cells taken on day 4, 6, 8, 10. Scale bar: 100 μm.

Supplemental Figure 5. SP^+ cells and $CD44^+$ cells sorted from ESCC cells display a higher sphere forming efficiency and express higher levels of pluripotency-associated factors. **(A)** Flow cytometry analysis of the $CD44^+$ population in the indicated cells. **(B)**

Number of spheres formed by SP^+ or SP^- cells (left panel) or $CD44^+$ or $CD44^-$ cells (right panel) sorted from the indicated ESCC cells. **(C)** Real-time PCR analysis of the mRNA expression levels of pluripotency-associated factors in the indicated cell populations. Error bars represent the mean ±SD of three independent experiments, * $P < 0.05$.

Supplemental Figure 6. AGK and JAK2 promote the $CD44^+$ population in ESCC. (A) Overexpression of AGK enhanced, whereas silencing AGK decreased, the $CD44^+$ population sorted from the indicated ESCC cells. **(B)** Silencing JAK2 decreased the $CD44^+$ population sorted from the indicated ESCC cells.

Supplemental Figure 7. JAK2-STAT3 signaling is required for the promoting effect of AGK on cancer stem cell-associated phenotypes. **(A)** Representative images of spheres formed by AGK overexpressing-cells infected with vector or JAK2 RNAi(s) taken on day 4, 6, 8, 10. Scale bar: 100 μm. **(B)** Silencing JAK2 decreased the $CD44^+$ population sorted from the indicated AGK-transduced ESCC cells. **(C)** Representative images of spheres formed by AGK overexpressing-cells infected with vector or STAT3 RNAi(s) taken on day 4, 6, 8, 10. Scale bar: 100 μm.

Supplemental Figure 8. Inhibition of JAK2 activity abrogates the ability of AGK to promote cancer stem cell-associated phenotypes. **(A** and **B)** Western blotting analysis of p-STAT3 (Tyr705) expression (A) or real-time PCR analysis of the expression of pluripotency associated markers (B) in the indicated cells treated with JAK2 inhibitor III (10 μM) for the indicated times. **(C** and **D)** Western blotting analysis of p-STAT3 (Tyr705) expression (C) and real-time PCR analysis of the expression of pluripotency associated markers (D) in the indicated cells treated with the indicated concentrations of JAK2 inhibitor III for 24 h. **(E** and **F)** Western blotting analysis of p-STAT3 (Tyr705) expression (E) and real-time PCR analysis of the expression of pluripotency associated markers (F) in the

indicated cells treated with JAK2 inhibitor II (100 μM) for the indicated times. **(G** and **H)** Western blotting analysis of p-STAT3 (Tyr705) expression (G) and real-time PCR analysis of the expression of pluripotency associated markers (H) in the indicated cells treated with the indicated concentrations of JAK2 inhibitor II for 16 h. α-tubulin was used as a loading control. Error bars represent the mean ±SD of three independent experiments, * $P < 0.05$.

Supplemental Figure 9. Expression of *AGK* mRNA is elevated in ESCC cell lines and tissues. (A) Real-time PCR analysis of *AGK* mRNA in 2 primary cultured human normal esophageal epithelial cells (NEECs) and 11 ESCC cell lines. **(B)** Real-time PCR analysis of *AGK* mRNA in 8 paired primary ESCC tissues (T) and the matched adjacent non-tumor tissues (ANT) from the same patient.

Supplemental Figure 10. AGK expression and JAK2-STAT3 activity correlate with the expression levels of pluripotency-associated factors in ESCC tissues. (A) Real-time PCR analysis of the mRNA expression of pluripotency-associated factors, including *ABCG2*, *SOX2*, *OCT4*, *NANOG*, *BMI1* and *CD44*, in 8 freshly collected human ESCC samples. **(B** and **C)** AGK expression (B) and JAK2-STAT3 activity (C) correlated significantly with the expression levels of pluripotency associated factors in freshly collected ESCC tissues. **(D)** GSEA plot showing that AGK levels positively correlated with the expression of pluripotency-associated factors, between normal and tumor tissues (left panel) and within tumor tissues (right panel), through an analysis of published ESCC patient profiles.

Supplemental Figure 11. AGK levels correlate with STAT3 activity in lung cancer and breast cancer datasets. (A-B) GSEA plot showing significant correlations between AGK expression and the STAT3-activated gene signatures (DAUER_STAT3_TARGETS_UP, V$STAT3_01/02) or STAT3-suppressed gene signatures (DAUER_STAT3_TARGETS_Dn) in published lung cancer gene expression profiles (statistic performed within tumor tissues

from GSE10245/19804/28571/31210, *n* = 464) (A) and breast patient gene expression profiles (statistic performed within tumor tissues from E-TABM-1186, *n* = 354) (B).

Supplemental Figure 12. Expression of IL6 does not correlate with STAT3 activation in clinical ESCC specimens. GSEA plot showing no significant correlation between IL6 expression and the STAT3-activated gene signatures (DAUER_STAT3_TARGETS_UP, V$STAT3_01/02) or STAT3-suppressed gene signatures (DAUER_STAT3_TARGETS_Dn) in published ESCC patient gene expression profiles (NCBI/GEO/GSE20347 and GSE29001, *n* = 79).

Supplemental Table 1. Clinicopathological characteristics and expression of AGK in ESCC patients

	Number of cases (%)
Gender	
Male	189(76.5)
Female	58(23.5)
Age (years)	
≦57	132(53.4)
>57	115(46.6)
Clinical stage	
I	36(14.6)
IIA	83(33.6)
IIB	32(13.0)
III	70(28.3)
IV	26(10.5)
T classification	
T1	36(14.6)
T2	63(25.5)
T3	138(55.9)
T4	10(4.0)
N classification	
N0	135(54.7)
N1	110(44.5)
N2	2(0.8)

M classification	
M0	221(89.5)
M1	26(10.5)
Tumor grade	
G1	76(30.8)
G2	107(43.3)
G3	64(25.9)
Vital status (at follow-up)	
Alive	82(33.2)
Death (tumor-related)	163(66.0)
Death (tumor-unrelated)	2(0.8)
Expression of AGK	
Low expression	127(51.4)
High expression	120(48.6)
Location	
Upper	22(8.9)
Middle	153(61.9)
Lower	72(29.1)
Therapy	
Surgery only	218(88.3)
CT or RT or CRT, +Surgery	29(11.7)
Recurrence or uncontrolled	
No	117(47.4)
Yes	130(52.6)

Supplemental Table 2. Correlations between AGK expression and clinicopathologic characteristics of ESCC patients

Characteristics		AGK		Chi-square test *P*-value
		Low No. cases (%)	High No. cases (%)	
Gender	Male	97(76.4)	92(76.7)	0.957
	Female	30(23.6)	28(23.3)	
Age (years)	≦57	66(52.0)	66(55.0)	0.633
	>57	61(48.0)	54(45.0)	
Clinical stage	I	27(21.3)	9(7.5)	<0.001
	IIA	53(41.7)	30(25.0)	
	IIB	15(11.8)	17(14.2)	
	III	29(22.8)	41(34.2)	
	IV	3(2.4)	23(19.2)	
T classification	T1	27(21.3)	9(7.5)	0.008
	T2	34(26.8)	29(24.2)	
	T3	63(49.6)	75(62.5)	
	T4	3(2.4)	7(5.8)	
N classification	N0	86(67.7)	49(40.8)	<0.001
	N1	40(31.5)	70(58.3)	
	N2	1(0.8)	1(0.8)	
M classification	M0	124(97.6)	97(80.8)	<0.001
	M1	3(2.4)	23(19.2)	
Tumor grade	G1	50(39.4)	26(21.7)	0.002
	G2	54(42.5)	53(44.2)	
	G3	23(18.1)	41(34.2)	

	Upper	13(10.2)	9(7.5)	
Location	Middle	74(58.3)	79(65.8)	0.453
	Lower	40(31.5)	32(26.7)	
Therapy	Surgery only	111(87.4)	107(89.2)	0.667
	CT or RT or CRT, +Surgery	16(12.6)	13(10.8)	
Recurrence or uncontrolled	No	70(55.1)	47(39.2)	0.012
	Yes	57(44.9)	73(60.8)	
Vital status	Alive	70(55.1)	12(10.0)	<0.001
	Death (tumor-related)	55(43.3)	108(90.0)	
	Death (tumor-unrelated)	2(1.6)	0(0.0)	

Supplemental Table 3. Univariate and multivariate analyses for 5-year overall survival

	Univariate analysis		Multivariate analysis		
	P	**Regression coefficient (SE)**	***P***	**Relative risk**	**95% confidence**
Clinical stage	<0.001	0.883(0.076)	0.002	1.547	1.167-2.051
Expression of AGK	<0.001	1.544 (0.173)	<0.001	3.764	2.617-5.412
T classification	<0.001	0.672(0.113)	0.062	1.298	0.987-1.708
N classification	<0.001	1.524(0.159)	0.004	1.954	1.233-3.097
M classification	<0.001	1.949(0.237)	0.097	1.737	0.904-3.338
Tumor grade	<0.001	0.429(0.107)	0.005	1.383	1.106-1.729
Location	0.428	-0.103(0.130)	0.774	1.043	0.784-1.387
Therapy	0.845	-0.046(0.234)	0.221	0.744	0.463-1.195

Supplemental Table 4. Univariate and multivariate analyses for 5-year disease-free survival

	Univariate analysis		Multivariate analysis		
	P	**Regression coefficient (SE)**	***P***	**Relative risk**	**95% confidence**
Clinical stage	<0.001	0.960(0.077)	<0.001	2.113	1.589-2.809
Expression of AGK	<0.001	1.510 (0.165)	<0.001	4.077	2.864-5.805
T classification	<0.001	0.678(0.109)	0.308	1.144	0.883-1.482
N classification	<0.001	1.559(0.152)	0.045	1.580	1.009-2.474
M classification	<0.001	1.873(0.234)	0.916	0.967	0.523-1.789
Tumor grade	<0.001	0.390(0.103)	0.016	1.302	1.051-1.614
Location	0.364	-0.114(0.125)	0.457	1.108	0.845-1.453
Therapy	0.952	0.014(0.228)	0.402	0.822	0.519-1.301

Supplemental Figure 1

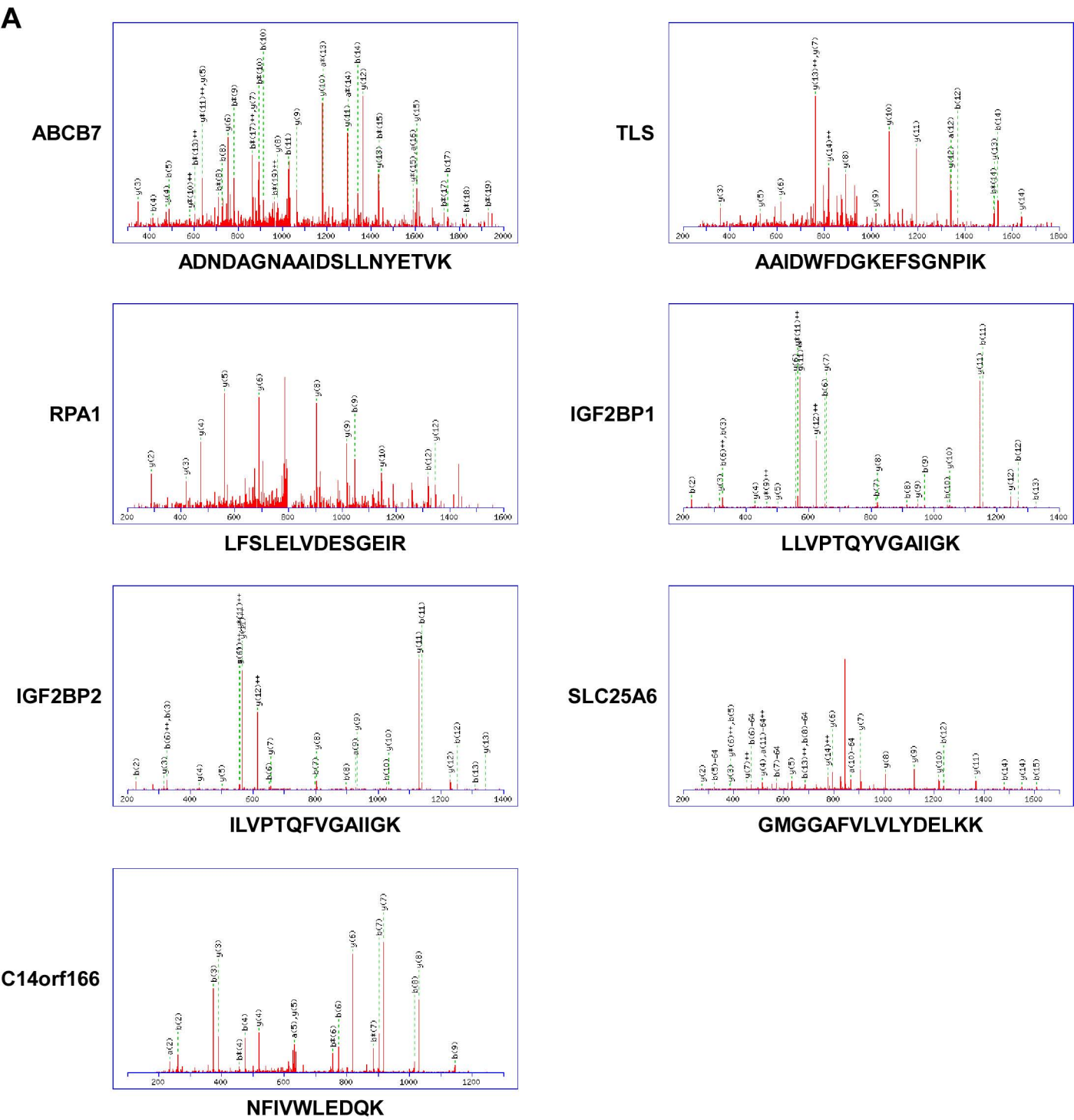

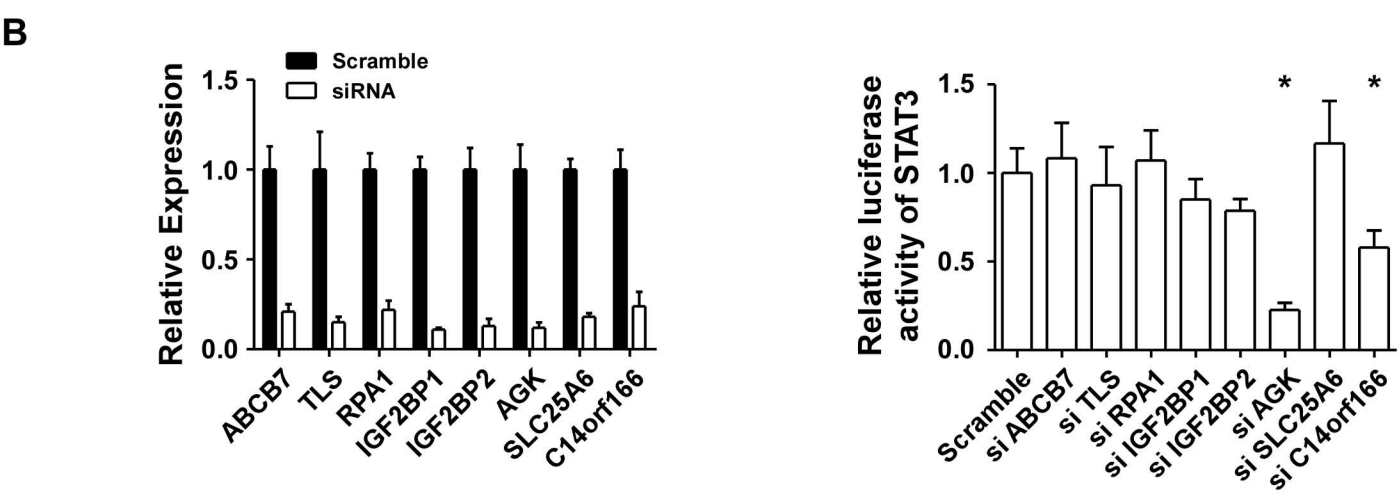

Supplemental Figure 1. Mass-spectrometric peptide sequencing of JH2-interacting proteins and identification of their effects on STAT3 transcriptional activity.

(A) Representative mass spectrometry plots and sequences of the peptides from potent JH2-interacting proteins identified from the JH2 precipitate presented in Figure 1A.

(B) Expression of mRNA and STAT3 luciferase reporter activity following silencing of potent JH2-interacting proteins identified from the JH2 precipitate presented in Figure 1A. Error bars represent the mean ± SD of three independent experiments, * $P < 0.05$.

Supplemental Figure 2

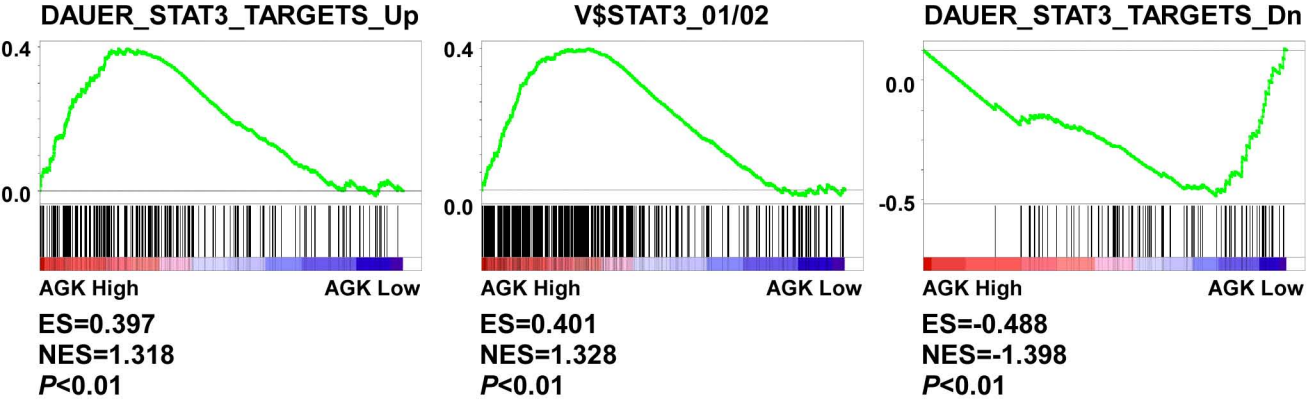

Supplemental Figure 2. AGK expression correlates with STAT3 activity in ESCC datasets. GSEA plot showing significant correlations between AGK expression and the STAT3-activated gene signatures (DAUER_STAT3_TARGETS_UP, V$STAT3_01/02) or STAT3-suppressed gene signatures (DAUER_STAT3_TARGETS_Dn) in a published cohort of ESCC gene expression profiles (statistic performed within tumor tissues from GSE20347/29001/33426, *n* = 109).

Supplemental Figure 3

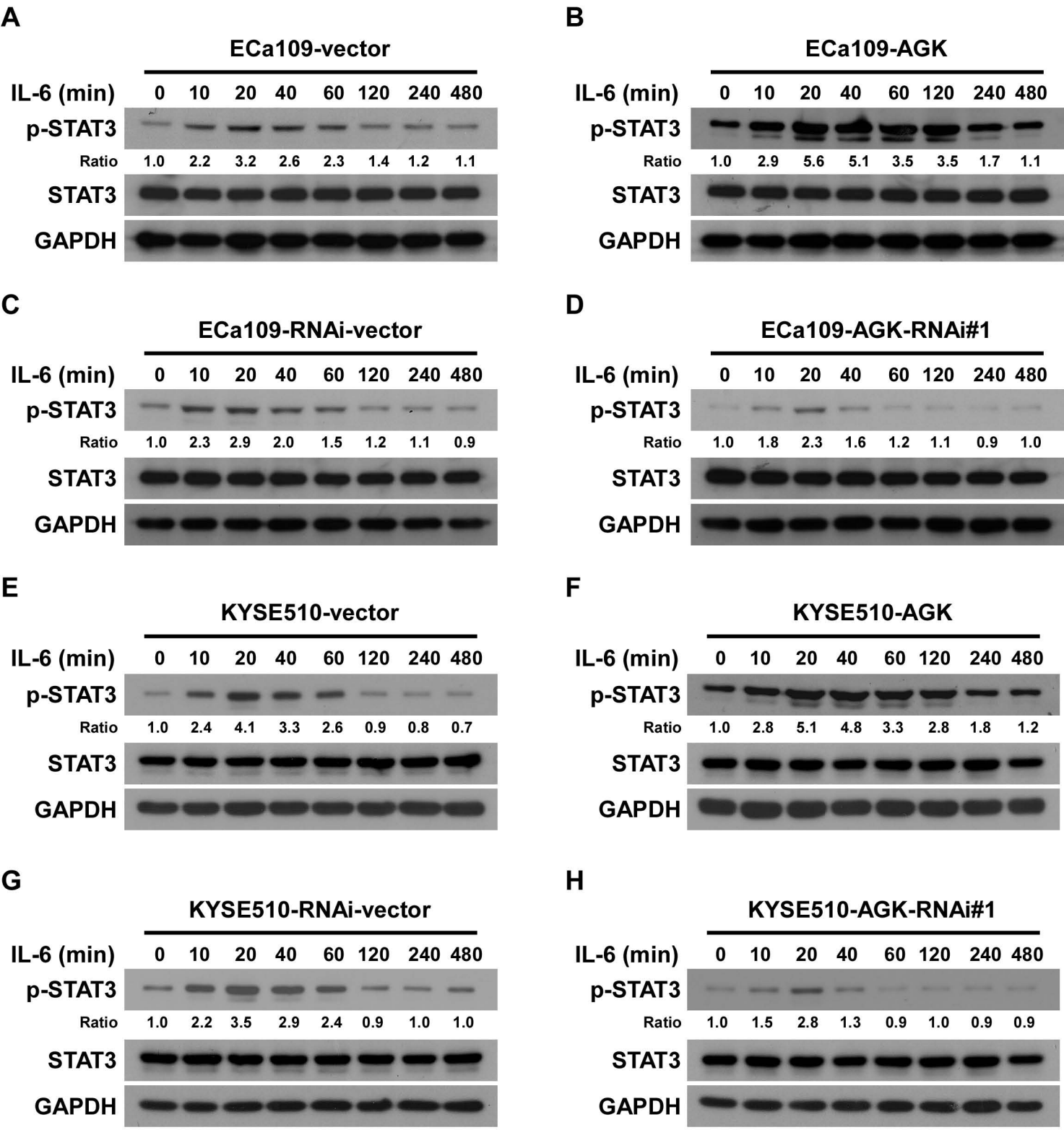

Supplemental Figure 3. Overexpression of AGK enhances the strength and duration of STAT3 activation.

(A-H) Western blotting analysis of the expression of p-STAT3 (Tyr705) and total STAT3 in the indicated cells treated with IL-6 (1 ng/ml) for various times (0-480 min). GAPDH was used as a loading control.

Supplemental Figure 4

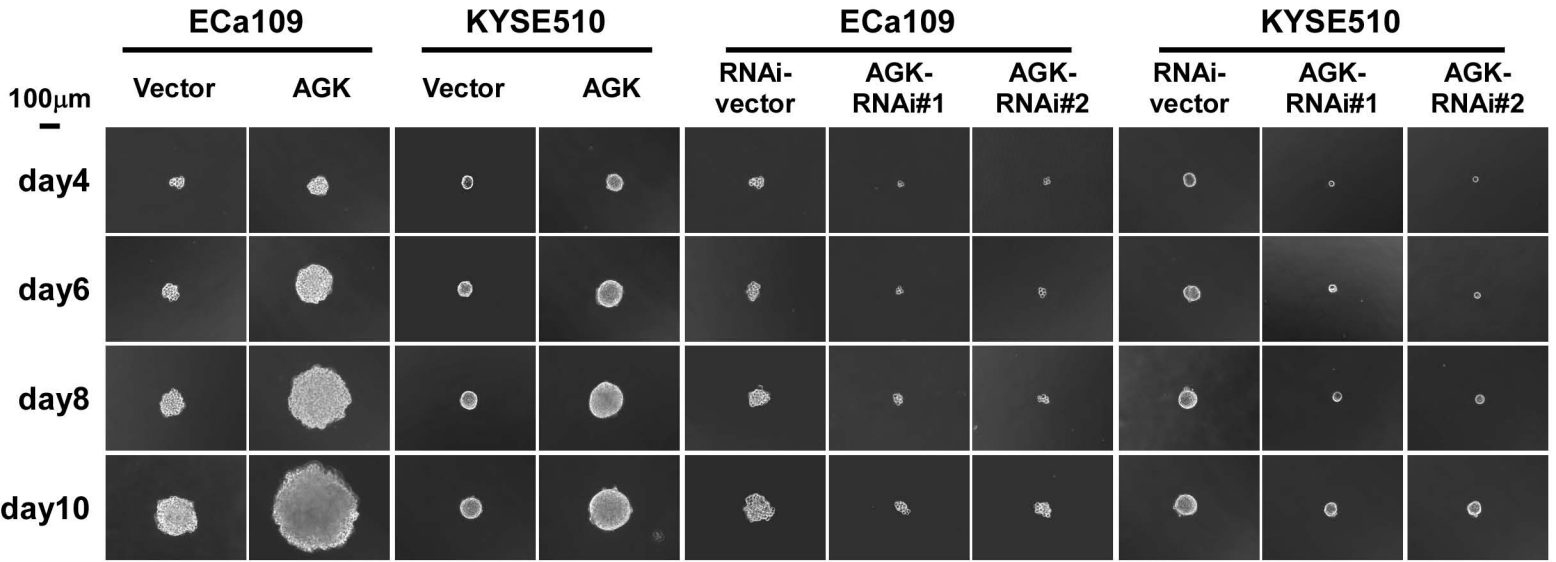

Supplemental Figure 4. AGK promotes the stem cell population and stem cell-like phenotype in ESCC. Representative images of spheres formed by AGK transduced- or AGK silenced-cells taken on day 4, 6, 8, 10. Scale bar: 100 μm.

Supplemental Figure 5

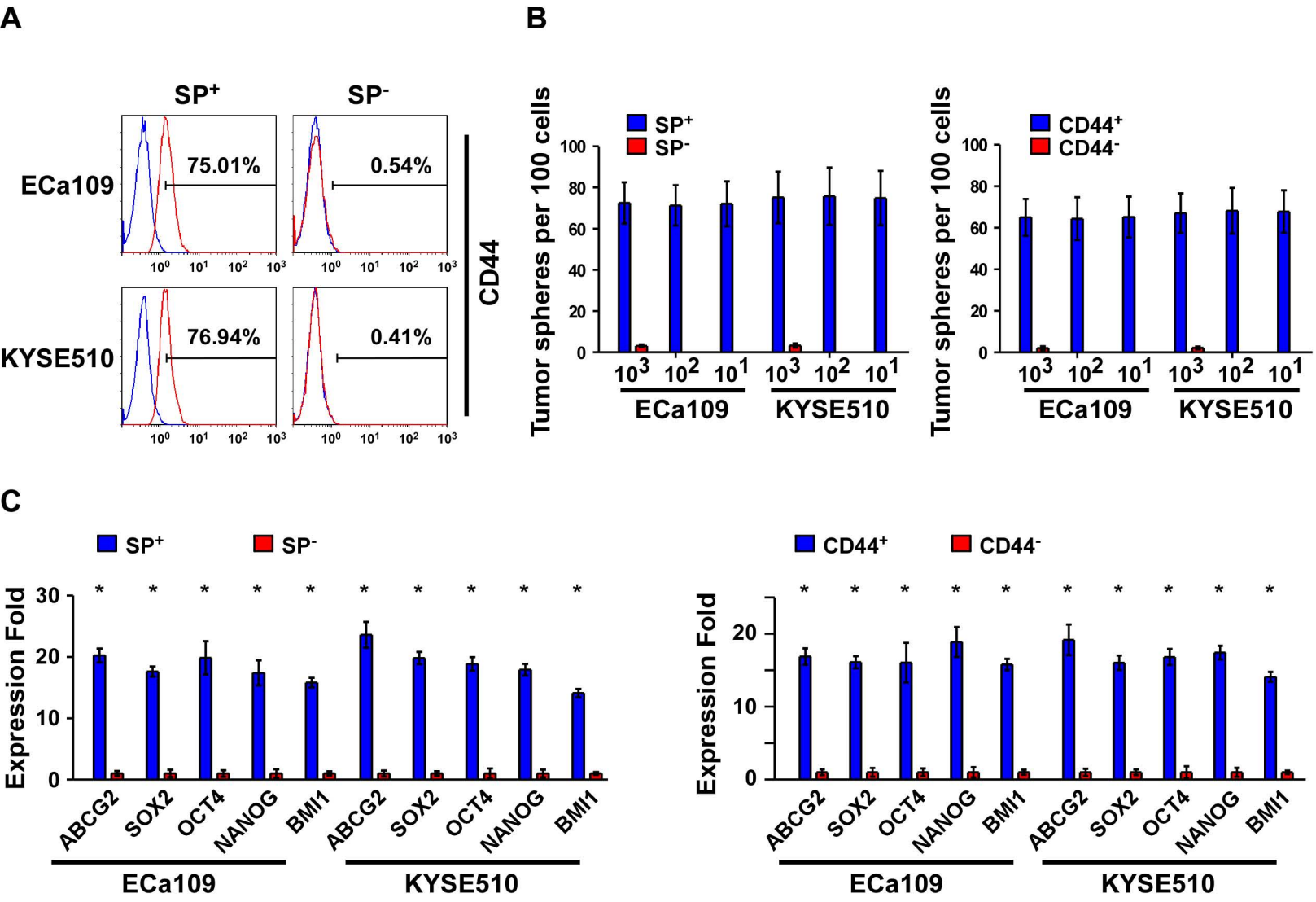

Supplemental Figure 5. SP$^+$ cells and CD44$^+$ cells sorted from ESCC cells display a higher sphere forming efficiency and express higher levels of pluripotency-associated factors.

(A) Flow cytometry analysis of the CD44$^+$ population in the indicated cells.

(B) Number of spheres formed by SP$^+$ or SP$^-$ cells (left panel) or CD44$^+$ or CD44$^-$ cells (right panel) sorted from the indicated ESCC cells.

(C) Real-time PCR analysis of the mRNA expression levels of pluripotency-associated factors in the indicated cell populations.

Error bars represent the mean ± SD of three independent experiments, * $P < 0.05$.

Supplemental Figure 6

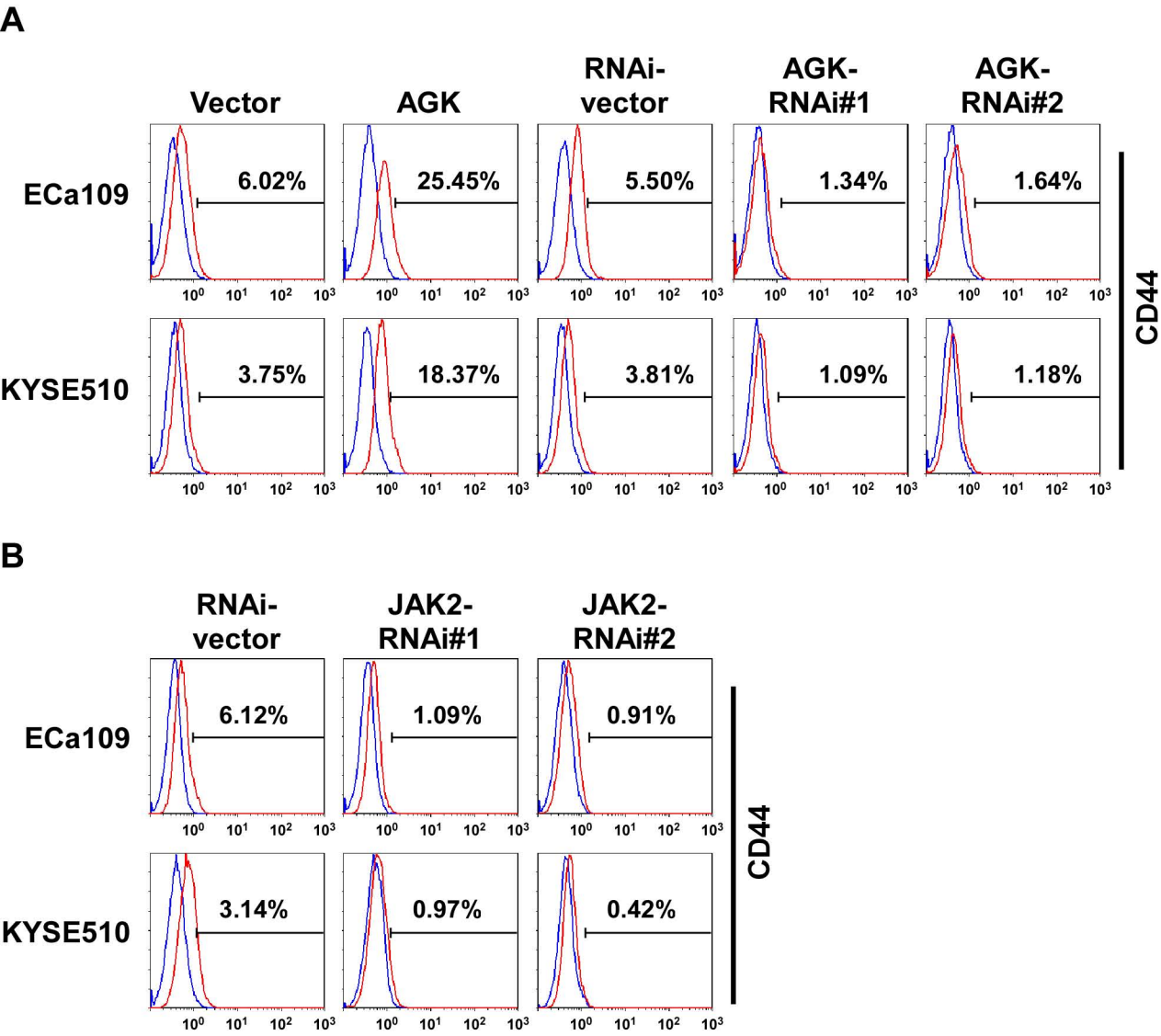

Supplemental Figure 6. AGK and JAK2 promote the CD44$^+$ population in ESCC.

(A) Overexpression of AGK enhanced, whereas silencing AGK decreased, the CD44$^+$ population sorted from the indicated ESCC cells.

(B) Silencing JAK2 decreased the CD44$^+$ population sorted from the indicated ESCC cells.

Supplemental Figure 7

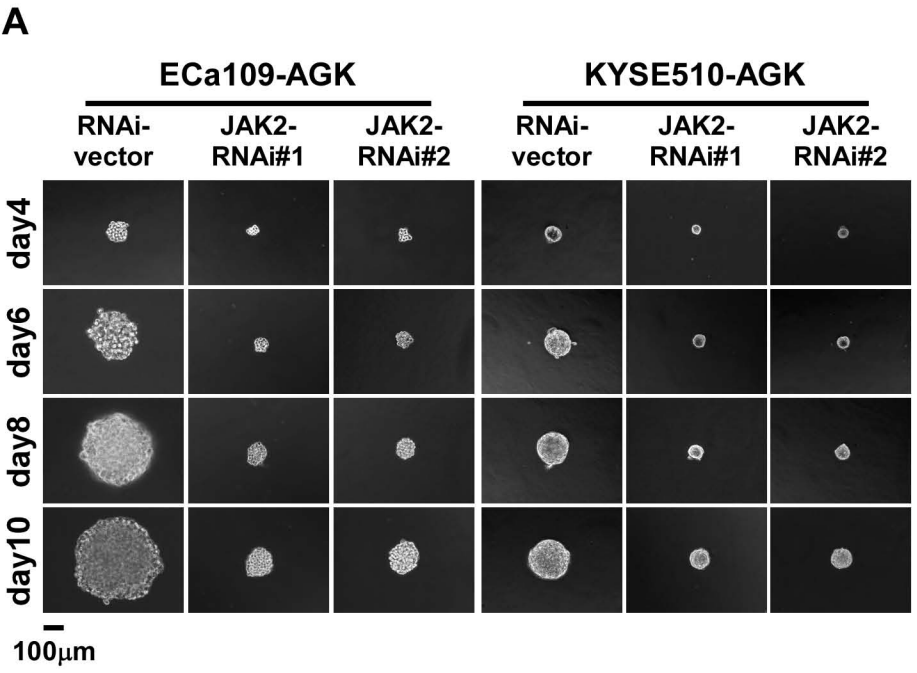

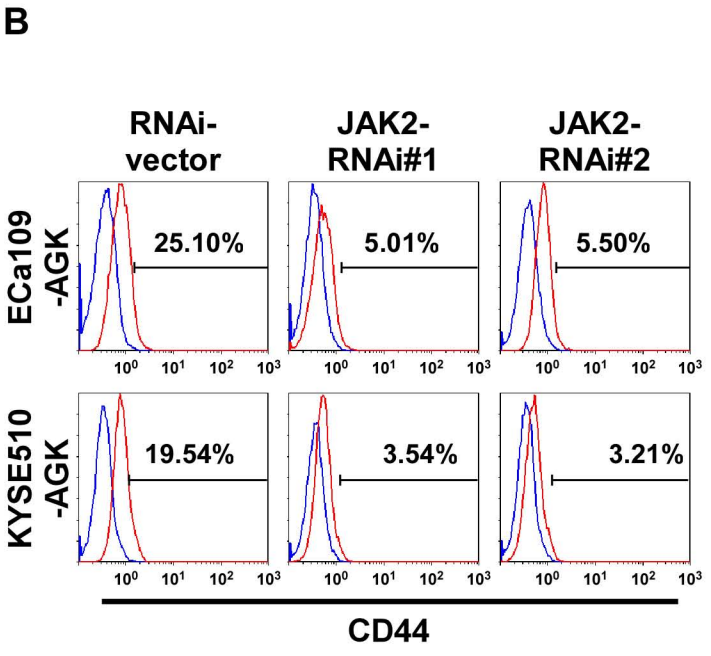

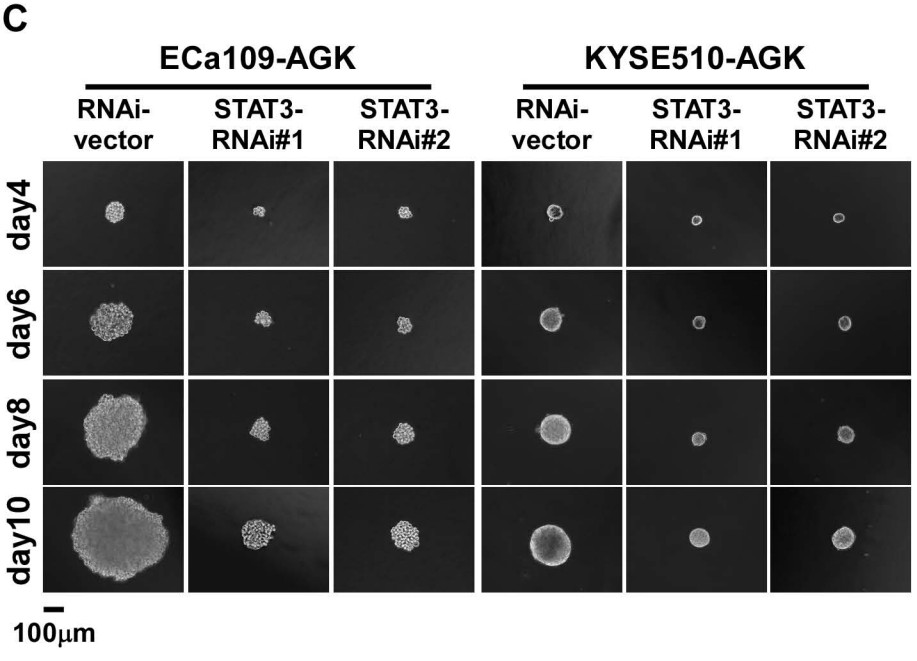

Supplemental Figure 7. JAK2-STAT3 signaling is required for the promoting effect of AGK on cancer stem cell-associated phenotypes.

(A) Representative images of spheres formed by AGK overexpressing-cells infected with vector or JAK2 RNAi(s) taken on day 4, 6, 8, 10. Scale bar: 100 μm.

(B) Silencing JAK2 decreased the $CD44^+$ population sorted from the indicated AGK-transduced ESCC cells.

(C) Representative images of spheres formed by AGK overexpressing-cells infected with vector or STAT3 RNAi(s) taken on day 4, 6, 8, 10. Scale bar: 100 μm.

Supplemental Figure 8

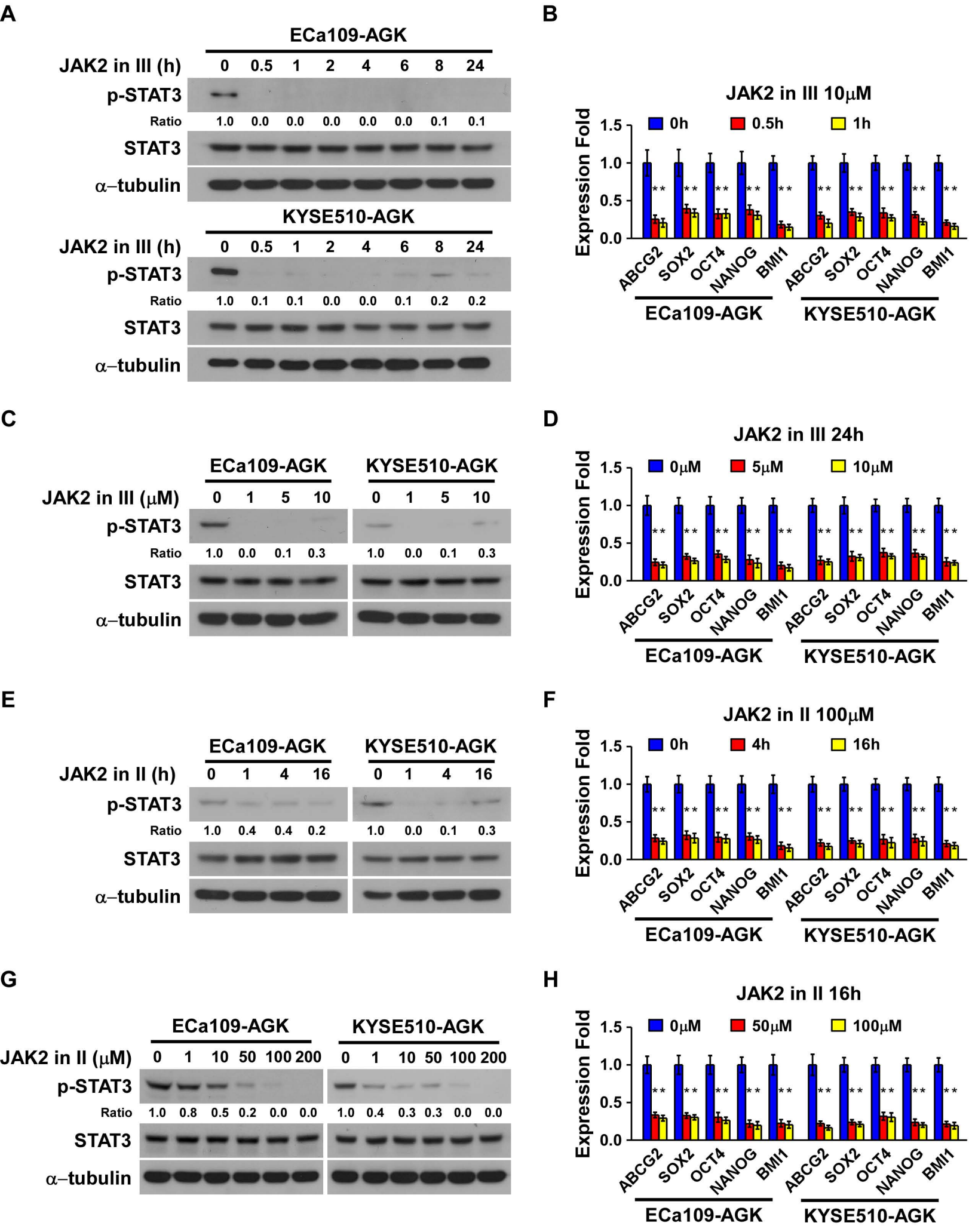

Supplemental Figure 8. Inhibition of JAK2 activity abrogates the ability of AGK to promote cancer stem cell-associated phenotypes.

(A and B) Western blotting analysis of p-STAT3 (Tyr705) expression (A) or real-time PCR analysis of the expression of pluripotency associated markers (B) in the indicated cells treated with JAK2 inhibitor III (10 μM) for the indicated times.

(C and D) Western blotting analysis of p-STAT3 (Tyr705) expression (C) and real-time PCR analysis of the expression of pluripotency associated markers (D) in the indicated cells treated with the indicated concentrations of JAK2 inhibitor III for 24 h.

(E and F) Western blotting analysis of p-STAT3 (Tyr705) expression (E) and real-time PCR analysis of the expression of pluripotency associated markers (F) in the indicated cells treated with JAK2 inhibitor II (100 μM) for the indicated times.

(G and H) Western blotting analysis of p-STAT3 (Tyr705) expression (G) and real-time PCR analysis of the expression of pluripotency associated markers (H) in the indicated cells treated with the indicated concentrations of JAK2 inhibitor II for 16 h.

α-tubulin was used as a loading control. Error bars represent the mean ± SD of three independent experiments, * $P < 0.05$.

Supplemental Figure 9

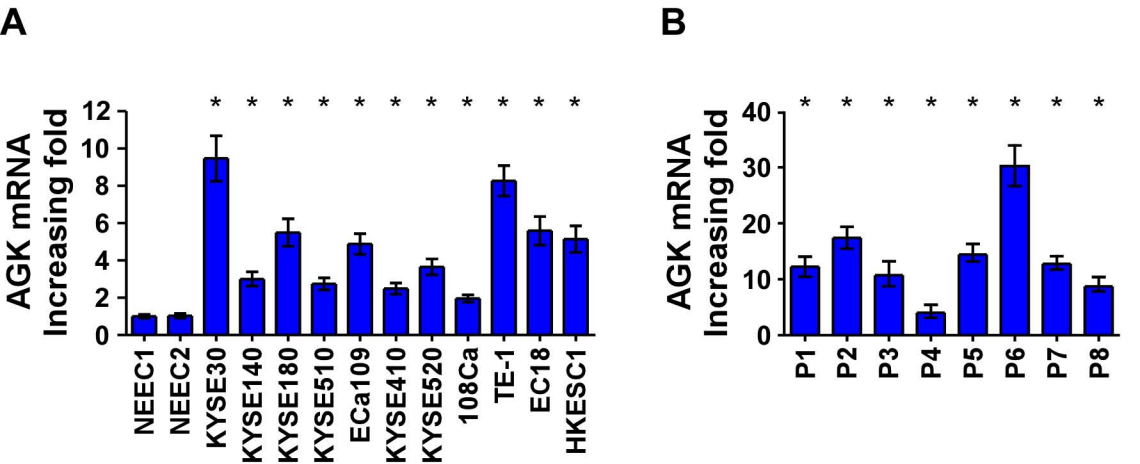

Supplemental Figure 9. Expression of AGK mRNA is elevated in ESCC cell lines and tissues.

(A) Real-time PCR analysis of AGK mRNA in 2 primary cultured human normal esophageal epithelial cells (NEECs) and 11 ESCC cell lines.

(B) Real-time PCR analysis of AGK mRNA in 8 paired primary ESCC tissues (T) and the matched adjacent non-tumor tissues (ANT) from the same patient.

Supplemental Figure 10

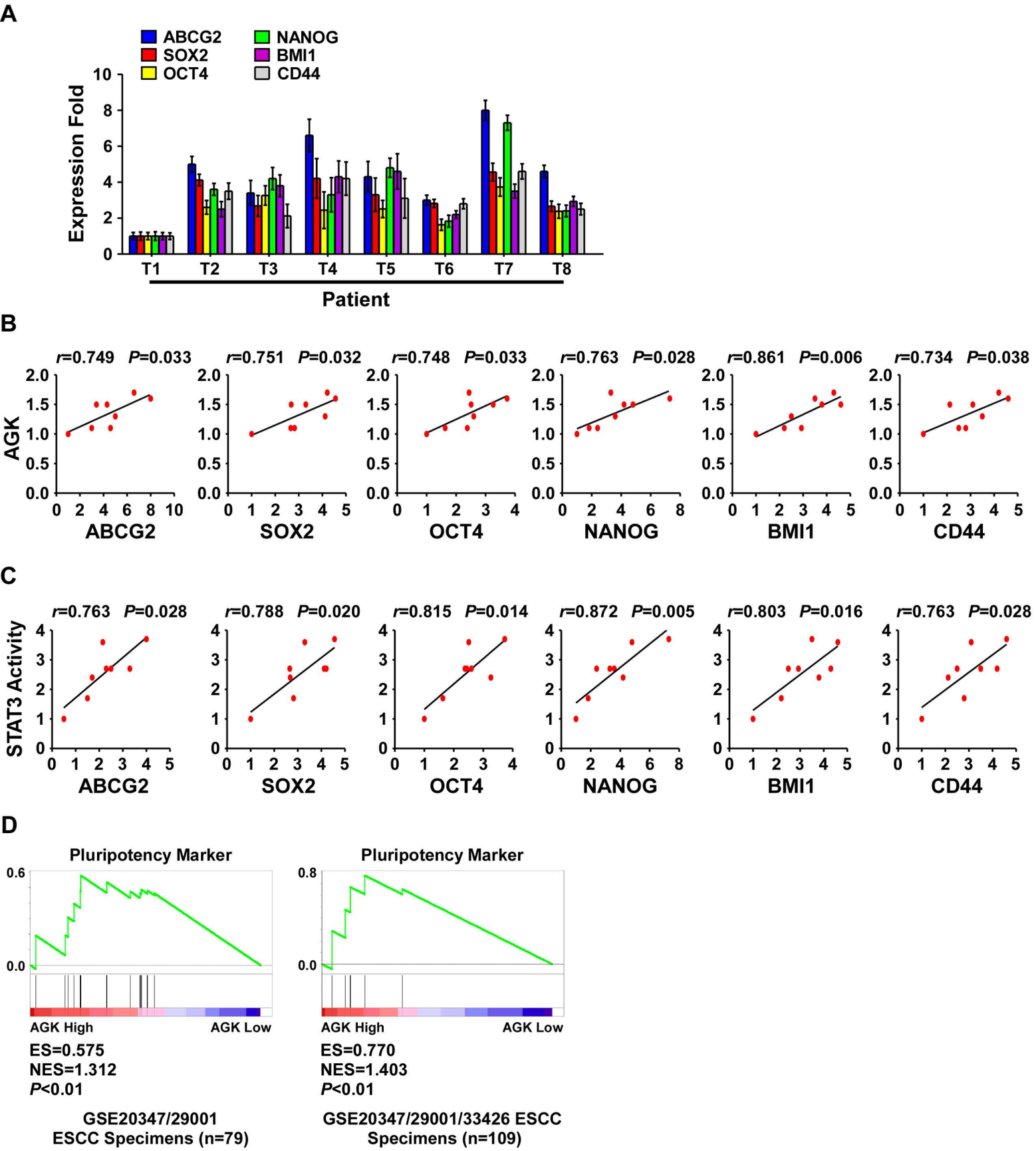

Supplemental Figure 10. AGK expression and JAK2-STAT3 activity correlate with the expression levels of pluripotency-associated factors in ESCC tissues.

(A) Real-time PCR analysis of the mRNA expression of pluripotency-associated factors, including *ABCG2*, *SOX2*, *OCT4*, *NANOG*, *BMI1* and *CD44*, in 8 freshly collected human ESCC samples.

(B and C) AGK expression (B) and JAK2-STAT3 activity (C) correlated significantly with the expression levels of pluripotency associated factors in freshly collected ESCC tissues.

(D) GSEA plot showing that AGK levels positively correlated with the expression of pluripotency-associated factors, between normal and tumor tissues (left panel) and within tumor tissues (right panel), through an analysis of published ESCC patient profiles.

Supplemental Figure 11

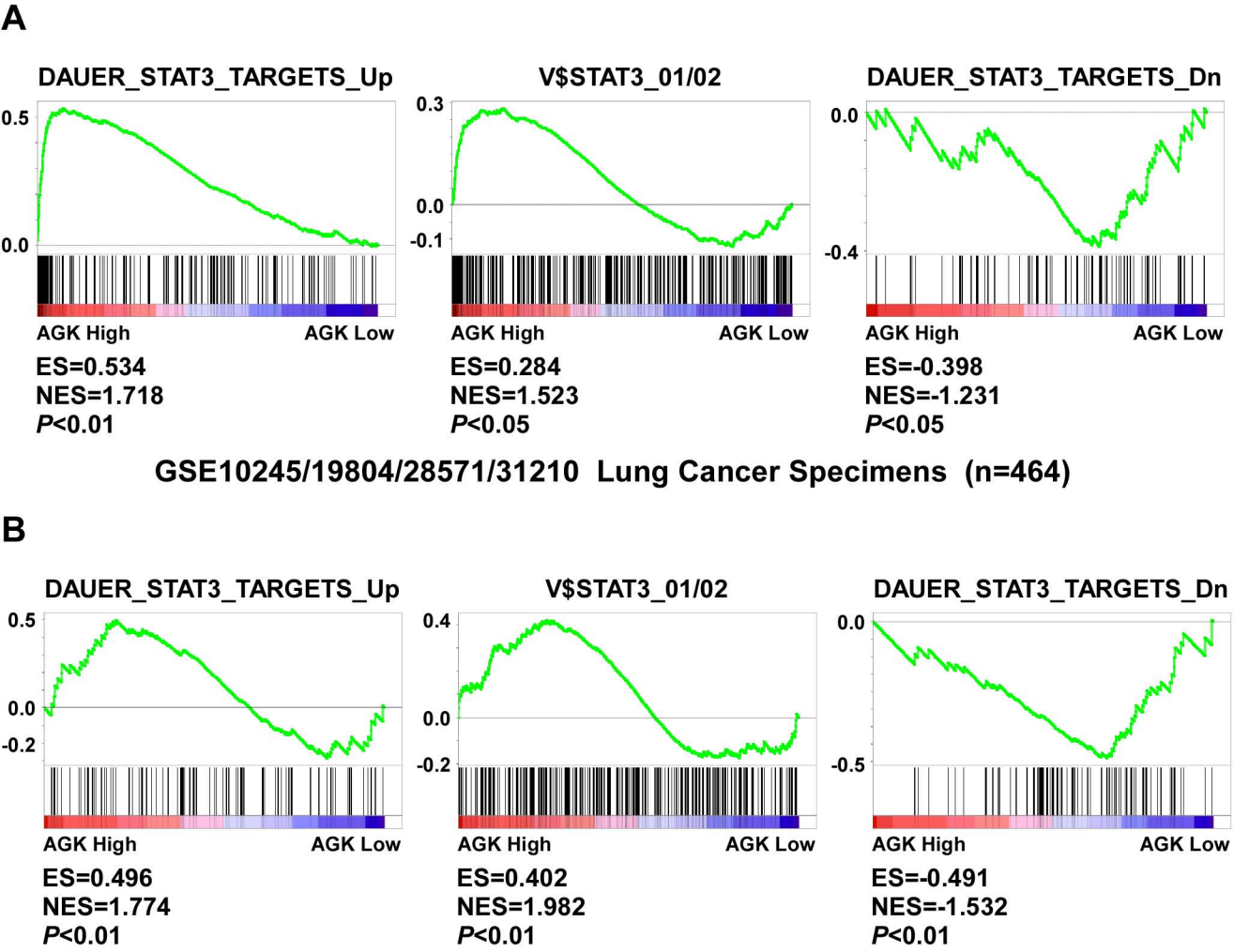

Supplemental Figure 11. AGK levels correlate with STAT3 activity in lung cancer and breast cancer datasets.

(A-B) GSEA plot showing significant correlations between AGK expression and the STAT3-activated gene signatures (DAUER_STAT3_TARGETS_UP, V$STAT3_01/02) or STAT3-suppressed gene signatures (DAUER_STAT3_TARGETS_Dn) in published lung cancer gene expression profiles (statistic performed within tumor tissues from GSE10245/19804/28571/31210, *n* = 464) (A) and breast patient gene expression profiles (statistic performed within tumor tissues from E-TABM-1186, *n* = 354) (B).

Supplemental Figure 12

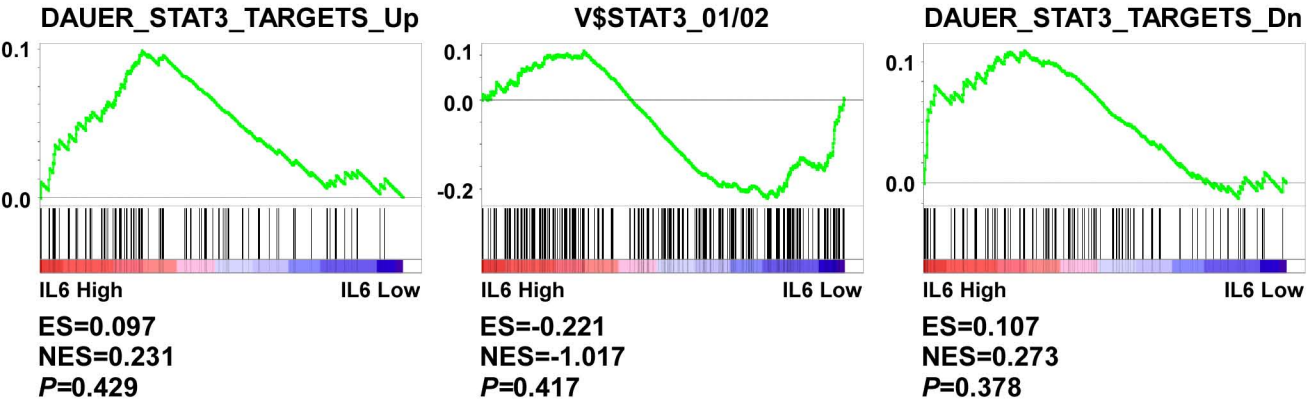

Supplemental Figure 12. Expression of IL6 does not correlate with STAT3 activation in clinical ESCC specimens.

GSEA plot showing no significant correlation between IL6 expression and the STAT3-activated gene signatures (DAUER_STAT3_TARGETS_UP, V$STAT3_01/02) or STAT3-suppressed gene signatures (DAUER_STAT3_TARGETS_Dn) in published ESCC patient gene expression profiles (NCBI/GEO/GSE20347 and GSE29001, *n* = 79).